Power Flow Coloring System over a Nano-Grid with Fluctuating Power Sources and Loads

Saher Javaid, Takekazu Kato, and Takashi Matsuyama

***Abstract*—Due to the excessive increase in environmental costs of non-renewable energy resources, there have been government legislation, policies, and new technologies to control carbon emissions. The increase in renewable resources requires new strategies for the operation and management of the electricity. This paper presents the power flow coloring system, which gives a unique ID to each power flow between a specific power source and a specific power load. It allows us to design multiple power flow patterns between distributed and fluctuating power sources and loads taking into account energy availability, cost, and carbon dioxide emission. For implementation, this paper proposes a cooperative distributed control method, where a master-slave role assignment scheme of power sources and a time-slot based feedback control are introduced to cope with power fluctuations while keeping the voltage stability. The experimental results clarify the practical feasibility of our proposed method in managing distributed fluctuating power sources and loads.**

***Index Terms*—Power flow coloring, Cooperative distributed control, i-Energy, Energy on demand, Nano-Grid**

I. Introduction

ACCORDING to the twenty-first session of conference of the parties (COP 21), global warming is declared as one of the major global issues to be solved. Due to the excessive increase in environmental costs of non-renewable resources, there have been regulations and international agreements to control CO2 emissions [1]. To encourage rapid and sustained development of renewable energy sources, Feed in Tariff (FiT) is already commercially implemented by utilities in some countries. FiT systems typically oblige electric utilities to purchase renewable generated power at fixed price per kWh [2]. Moreover, the installation cost of renewable technologies is rapidly decreasing during recent years and slowly approaching grid parity (cost of generated power from alternative power source i.e., PV is equal to price of purchasing power from grid) [3]. The expiration of FiT and decreasing costs for PV systems make an attractive choice for households and small communities to intentionally disconnect from the utility grid and start producing and consuming their own electricity [4].

Taking into account current market trends and future opportunities, major growth in small-scale power generation systems (PGSs) is observed. This is mainly because residential and commercial areas represent a major part of power consumption and carbon dioxide emissions and partly because small-scale photovoltaics, wind turbines, fuel cells, and storage batteries have been introduced into houses, factories, and in offices. The large scale penetration of small-scale PGSs results in drastic change in structure of residential and commercial areas [5].

Nano-grid (NG) [6] is an example for such changing structures which includes multiple power generating sources, energy storage facilities and in-house power distribution system and a variety of appliances. NGs have been studied significantly for future power distribution architecture from tens of kW to MW leading to the micro-grid (MG) level [7] and often operate over a simple shared power line. Moreover, a NG can be designed independently or can be associated with the national grid either for AC or DC power management [8]. As a NG is usually affiliated with MG or national grid, it have less problems as compare to national wide grid in handling frequency stability, power loss, and reactive power.

In [9]–[11], the concept of the Power Flow Coloring is proposed, which attaches the unique identification to each power flow between a pair of power source and load. Though, the concept of the power flow coloring could be applied to any type of power grid, this paper particularly focuses on a NG. The reason is, the basic technologies can be developed for the implementation of the power flow coloring and facilitated in a NG consisting of a shared bus power line without complicated structures of power transmission and distribution.

The power flow coloring can manage multiple power flow streams with diverse characteristics. For example, unpredicted generated power by photovoltaics can be directly flow into a power load such as coolers/heaters without using storage buffers. The utilization of renewable sources can help in reducing the gas emissions. Moreover, the power flow coloring can assist in recognizing the cost effective usage of power from different power sources. In our previous paper [11], the implementation of the power flow coloring over a NG was presented which focused on fluctuating loads and fluctuating power source management is kept for future studies. While this paper gives a complete power flow coloring system over a NG with fluctuating power sources and loads while keeping the voltage stable. The rest of the paper is organized as follows; Section II surveys related works, and implementation methods of the power flow coloring. Section III shows representation and compilation of a power flow pattern between multiple power devices. In section IV, we propose a agent based cooperative distributed system architecture. Section V introduces system protocol with master-slave role assignment for power source agents and the time-slot based feedback control to cope

Saher Javaid is affiliated with the Research Unit for Smart Energy Management, Center for the Promotion of Interdisciplinary Education and Research, Kyoto University, Kyoto, Japan, E-mail: saherjavaid@i.kyoto-u.ac.jp

Takekazu Kato is affiliated with the Department of Electrical and Electronic Engineering, Faculty of Science and Technology, Shizuoka Institute of Science and Technology, Japan Email: t.kato@ieee.org

Takashi Matsuyama is affiliated with the Graduate School of Informatics, Kyoto University, Kyoto, Japan Email: tm@i.kyoto-u.ac.jp

Manuscript received April 19, 2005; revised August 26, 2015.

with power fluctuations. In Section VI, the practicality of the power flow coloring system is demonstrated with experimental results. Section VII gives concluding remarks.

II. Related Works

The electricity market is experiencing significant changes because of large scale integration of renewable energy resources from distribution level down to individual household.

The transactive energy (TE) [12] has received much attention and has been a part of many discussions these days. The TE is defined as a system of control and economic mechanisms which enables the dynamic balance of power supply and power demand across the entire electrical infrastructure. The growing penetration of rooftop PV systems bring both the variability of power supply and a need for utilities to coordinate increasing number of variable loads to maintain a balanced and reliable system [13]. Our proposed power flow coloring system could be one of the possible solutions in near future.

Some readers might recognize similarities between the consignment power supply and the power flow coloring system but both are different. Firstly, the former handles volumes of power and real-time power control is not required. The latter, controls instantaneous power. Secondly, no explicit control is introduced for consignment supply because amount of power is far less than power manage, however, power flow coloring managed power over a NG of similar amount. That is, a sophisticated stability control mechanism should be developed. Thirdly, the power flow coloring can manage dynamically fluctuating sources and loads, which is out of scope of consignment power supply. In last, power flow coloring can manage power flows from multiple power sources to one load.

There are many implementation methods of the power flow coloring system classified as: power line switching, power routing, and synchronised source-load control. In [14], Yasuo et al. proposed a matrix power line switch between a group of power sources and a group of loads. A physical power line connection is established between a power source and a load. While its control is simple, only one-to-one connection between a power source and a load can be realized and hard to scale up if the number of nodes grows. Tsuguhiro et al. [15] and Rikiya et al. [16] proposed power routing methods. They developed so-called power routers which receive, store, and transmit chunks of power, power packets, just in the same way as message packet routers: a chunk of power is associated with source ID and destination ID. By introducing a multiplexing method, a simple power line can support multiple power packet transmissions. For realization, each router should be equipped with storage, which requires mass investments for the routing methods to be implemented in the existing grid.

The cooperative distributed control method for the power flow coloring system can be categorised as synchronized source-load control method, which can be used inside a household and also for local community in a NG without much investments. Moreover, it manages power fluctuations of power sources and loads by controlling terminal devices in real-time, which is the technical advantage of our proposed method. For implementation, we introduce a cooperative distributed system consisting of power managers, power source agents, and load agents, which communicate with each other for the realization of the power flow coloring.

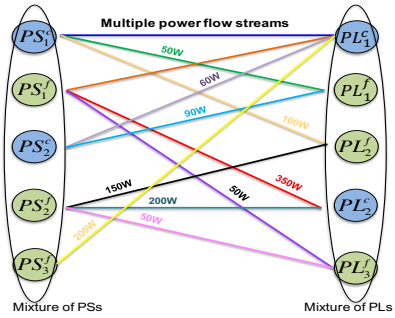

Fig. 1: Representation of a PFP.

III. Representation and Compilation of a Power Flow Pattern (PFP)

This section shows representation and compilation of a PFP between multiple power sources (PSs) and power loads (PLs). A PS can supply electric power e.g. solar panel, wind turbine, utility grid etc. and a PL consumes electric power supplied by PS(s). Both power devices (PSs/PLs) are classified into two categories i.e., *controllable* and *fluctuating* based on their types, characteristics, and functionalities. A controllable PS/PL can control its power (supply/consume) against power fluctuations whereas, fluctuating PS/PL cannot control its power. All controllable and fluctuating power devices are considered with unique identifiers.

For example, all PSs (controllable and fluctuating) are indexed as PS_i^c $(i \in \{1, 2, \cdots, I\})$ and PS_j^f $(j \in \{1, 2, \cdots, J\})$, respectively. Where, I and J represent total no. of controllable PSs and fluctuating PSs. Similarly, all PLs comprising of controllable and fluctuating are represented with unique identifiers such as PL_k^c $(k \in \{1, 2, \cdots, K\})$ and PL_l^f $(l \in \{1, 2, \cdots, L\})$. Where, K and L show total no. of controllable PLs and fluctuating PLs. A power flow is defined as power flowing from a specific type of a PS to a specific type of PL(s). Each power flow is associated with some power level in Watt. A power flow pattern (PFP) consists of multiple power flow streams between PSs and PLs, which can be represented by a colored bipartite graph (see Fig. 1). All power devices with both types are represented with different color. It is also possible to represent a PFP with a matrix notation arranged in combination of multiple rows and columns. The rows and columns of the given matrix denote PSs and PLs (both types). Each element of given matrix is referred to a nominal power level in Watt supplied from particular type of PS to specified PL. For example, P_{IK}^{cc} shows power flow from Ith controllable PS to Kth controllable PL, P_{IL}^{cf} denotes power flow from Ith controllable PS to Lth fluctuating PL, P_{JK}^{fc} represents power flow from Jth fluctuating PS to Kth controllable PL, and P_{JL}^{ff} shows power flow from Jth fluctuating PS to Lth fluctuating PL. Here, we assumed that given PFP satisfies all constraints on power supply and consumption and a consistent and realizable PFP is designed by the system.

After matrix representation, compilation of PFP matrix starts. The compilation of a PFP is defined as a process which uses given PFP matrix and measured power levels of fluctuating power devices to computes power levels for controllable power devices under the power balance constraint such that the total power supply from a PS is equal to the total power consumption of PLs attached with that particular PS.

PFP=

$$\begin{array}{c|cccc|cccc} & PL_1^c & PL_2^c & \cdots & PL_K^c & PL_1^f & PL_2^f & \cdots & PL_L^f \\ PS_1^c & P_{11}^{cc} & P_{12}^{cc} & \cdots & P_{1K}^{cc} & P_{11}^{cf} & P_{12}^{cf} & \cdots & P_{1L}^{cf} \\ PS_2^c & P_{21}^{cc} & P_{22}^{cc} & \cdots & P_{2K}^{cc} & P_{21}^{cf} & P_{22}^{cf} & \cdots & P_{2L}^{cf} \\ \vdots & \vdots & \vdots & \ddots & \vdots & \vdots & \vdots & \ddots & \vdots \\ PS_I^c & P_{I1}^{cc} & P_{I2}^{cc} & \cdots & P_{IK}^{cc} & P_{I1}^{cf} & P_{I2}^{cf} & \cdots & P_{IL}^{cf} \\ \hline PS_1^f & P_{11}^{fc} & P_{12}^{fc} & \cdots & P_{1K}^{fc} & P_{11}^{ff} & P_{12}^{ff} & \cdots & P_{1L}^{ff} \\ PS_2^f & P_{21}^{fc} & P_{22}^{fc} & \cdots & P_{2K}^{fc} & P_{21}^{ff} & P_{22}^{ff} & \cdots & P_{2L}^{ff} \\ \vdots & \vdots & \vdots & \ddots & \vdots & \vdots & \vdots & \ddots & \vdots \\ PS_J^f & P_{J1}^{fc} & P_{J2}^{fc} & \cdots & P_{JK}^{fc} & P_{J1}^{ff} & P_{J2}^{ff} & \cdots & P_{JL}^{ff} \end{array}$$

Here, it is assumed that there are no communication and computation delays. As the physical power by a fluctuating power device varies a lot due to its nature and operation modes, the nominal power value specified in PFP matrix is hard to maintain physically. Therefore, there is a need to design a compilation algorithm which can (i) link between physical power levels by power devices and nominal power levels in PFP matrix as well as (ii) manage all possible power flow streams between PSs and PLs (with both types).

Our idea to devise the compilation algorithm is that the PFP matrix can be partitioned into following 4 disjoint sectors, each of which can be processed independently of the others. The 4 disjoint sectors are listed below,

1) PFP between controllable PSs and controllable PLs
2) PFP between controllable PSs and fluctuating PLs
3) PFP between fluctuating PSs and controllable PLs
4) PFP between fluctuating PSs and fluctuating PLs

Here, "independent" refers to compilation of each sector that ensures its independent compilation process. Each sector has its own sub-algorithm for compilation which computes power levels for controllable power devices. This means the computation of power levels for controllable power devices in each sector is a partial computation of power for controllable power devices and overall power of particular controllable power device can be achieved by summing up all partial computations during each sector's compilation process. Therefore, it is required to initialize the power levels of all controllable power devices (PSs/PLs) because during compilation process controllable power devices will receive target power level for power supply/consumption.

For example, the power supply of ith controllable PS and power consumption by kth controllable PL are initialized. The following initialization algorithm is required to initialize power levels of all attached controllable power devices. The compilation sub-algorithms for each sector of given PFP matrix are discussed in the following subsections.

Algorithm 1 Initialization of all controllable power PSs, (PS_i^c), and PLs, (PL_k^c)

for $i = 1$ to I **do**
  for $k = 1$ to K **do**
    $W(PS_i^c) = W(PL_k^c) = 0$
  end for
end for

A. PFP between controllable PSs and PLs

The compilation sub-algorithm of first sector of PFP matrix is related with power flow streams between controllable PSs and controllable PLs only. Since all power devices are controllable, the power supply from PSs and power consumption by PLs can be controlled accurately according to the nominal power levels in Watt specified. The given sub-algorithm

Algorithm 2 For power flow streams between PS_i^c and PL_k^c

for $i = 1$ to I **do**
  for $k = 1$ to K **do**
    $W(PS_i^c) = P_{ik}^{cc} + W(PS_i^c)$
    $W(PL_k^c) = P_{ik}^{cc} + W(PL_k^c)$
  end for
end for

computes power levels for controllable power devices. For example, specified power level in PFP matrix as, P_{ik}^{cc}, is added to the total power supply of ith controllable PS, $W(PS_i^c)$, and total power consumption of kth controllable PL, $W(PL_k^c)$.

B. PFP between controllable PSs and fluctuating PLs

The sub-algorithm of second sector of the PFP matrix considers the power flow streams between controllable PSs and fluctuating PLs.

It is possible that fluctuating PL of this sector is further connected with fluctuating PS(s). In this case, the fluctuating PL with all power flow streams will be eliminated from the compilation process of second sector (see Fig. 2). These eliminated power flow streams would be compiled together with the sector 4 of the PFP matrix, which will be explained later. This means that the target power flow streams that can be handled with this sub-algorithm consists of power flow streams between controllable PSs and fluctuating PLs only.

As it is well known that the power consumption of fluctuating PLs fluctuates and sometimes varies a lot due to its operation modes (e.g., automatic power control in an air-conditioner). This means the nominal power value specified in PFP matrix is just a reference and hard to maintain physically. To associate nominal power level given in PFP matrix with physical power values of fluctuating PL, elements of sector 2 of PFP matrix are converted to power ratios called *Power Supply Ratio (PSR)*. The *PSR* can be computed as,

$$PSR = \left[R_{il}^{cf}\right] = \left[\frac{P_{il}^{cf}}{\sum_{i=1}^{I} P_{il}^{cf}}\right] \quad (1)$$

$$\sum_{i=1}^{I} R_{il}^{cf} = 1 \text{ for all } l,$$

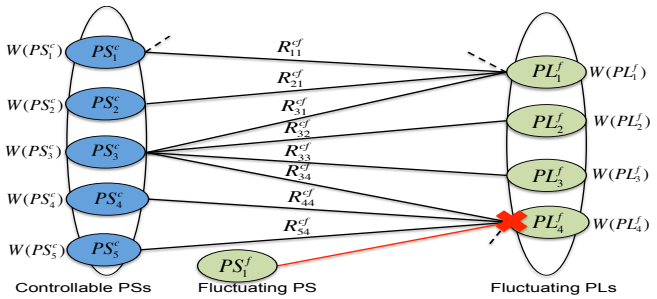

Fig. 2: Target power flow streams for compilation process of sector 2 of PFP matrix

Where, P_{il}^{cf} and R_{il}^{cf} denote the nominal power level and *PSR* supplied from ith controllable PS to lth fluctuating.

Algorithm 3 For power flow streams between PS_i^c and PL_l^f

for $i = 1$ to I **do**
  for $l = 1$ to L such that for all $j = 1$ to J, $P_{jl}^{ff} = 0$ **do**
    $W(PS_i^c) = R_{il}^{cf} \cdot W(PL_l^f) + W(PS_i^c)$
  end for
end for

The given sub-algorithm for compilation of sector 2 of PFP matrix computes power levels for controllable PSs, $W(PS_i^c)$, when measured power consumption levels of fluctuating PLs, $W(PL_l^f)$, and PFP are given. The ratio based power levels of fluctuating PLs are added to the power supply of all controllable PSs, which supply power to those PLs. The target power flow streams are checked by, $P_{jl}^{ff} = 0$, which shows no power flow streams between fluctuating power devices exist in this compilation process.

C. PFP between fluctuating PSs and controllable PLs

The compilation of third sector of PFP matrix is related with power flow streams between fluctuating PSs and controllable PLs. It is possible that the fluctuating PS of this sector is further attached with fluctuating PL(s). The same situation is discussed in previous subsection already that power flow streams between fluctuating power devices would be compiled together with the compilation process of sector 4. Thus, the target power flow streams that can be solved by the sub-algorithm of this sector consists of fluctuating PSs and controllable PLs only. Due to the nature of fluctuating PSs e.g., PV, the generated power is not constant and stable. To deal with fluctuating generated power, the nominal power levels of sector 3 are converted to power ratios called *Power Consumption Ratio (PCR)* for controllable PLs. The *PCR* can be computed as,

$$PCR = \left[R_{jk}^{fc}\right] = \left[\frac{P_{jk}^{fc}}{\sum_{k=1}^{K} P_{jk}^{fc}}\right] \tag{2}$$

$$\sum_{k=1}^{K} R_{jk}^{fc} = 1 \text{ for all } j,$$

Where, P_{jk}^{fc} and R_{jk}^{fc} denote nominal power level and *PCR* consumed by kth controllable PL supplied from jth fluctuating PS. The power level for controllable PLs can be computed with given sub-algorithm when PFP matrix and measured power supply levels of fluctuating PSs, $W(PS_j^f)$ are given.

Algorithm 4 For power flow streams between PS_j^f and PL_k^c

for $k = 1$ to K **do**
  for $j = 1$ to J such that for all $l = 1$ to L, $P_{jl}^{ff} = 0$ **do**
    $W(PL_k^c) = R_{jk}^{fc} \cdot W(PS_j^f) + W(PL_k^c)$
  end for
end for

D. PFP between fluctuating PSs and PLs

The compilation of last sector of PFP matrix includes power flow streams between fluctuating devices and power flow streams eliminated from the compilation processes of sector 2 and 3, respectively. Since the power flow streams consists of fluctuating power devices only, it is not possible to maintain the nominal power levels specified in PFP matrix.

One idea to control flow of power between fluctuating power devices is to ask cooperation from controllable power devices. As these power flow streams cannot be controlled by fluctuating power devices alone, the support from controllable power devices can make it possible to control the power fluctuations of fluctuating power devices (PS^f/PL^f). This idea implies a constraint that each fluctuating power device of the power flow, must be directly attached with at least one controllable power device otherwise it is not possible to control power supply or consumption of the fluctuating device.

For example, for a power flow from a fluctuating PS to a fluctuating PL, each fluctuating power device on both sides of the power flow must be directly attached with at least one controllable power device (see Fig. 3). Then, attached controllable power devices on both sides of the power flow can control the power fluctuations of fluctuating power devices. This means compilation of this sector involves both types of power devices (i.e., controllable and fluctuating) on each side of a power flow. This makes the compilation of this sector *"Global"*. That is, compilation of this sector should be done together with other sectors of PFP matrix. For this reason, sector 2 and 3 should be re-compiled and ratio matrices need revision with global aspect. The re-computation of power ratios are named as *Global Power Supply Ratio (GPSR)* and *Global Power Consumption Ratio (GPCR)*.

Since computation of *GPSR* considers both types of PSs with fluctuating PLs i.e., sector 2 and sector 4 while neglecting sector 3. The computation consists of two ratios; the first ratio, R_{il}^1, is used for sector 2, and second ratio, R_{jl}^2 is applied on sector 4 of the PFP matrix.

$$GPSR = \begin{bmatrix} R_{il}^1 \\ R_{jl}^2 \end{bmatrix} \tag{3}$$

$$R_{il}^1 = \left[\frac{P_{il}^{cf}}{\sum_{i=1}^{I} P_{il}^{cf} + \sum_{j=1}^{J} P_{jl}^{ff}}\right] \tag{3a}$$

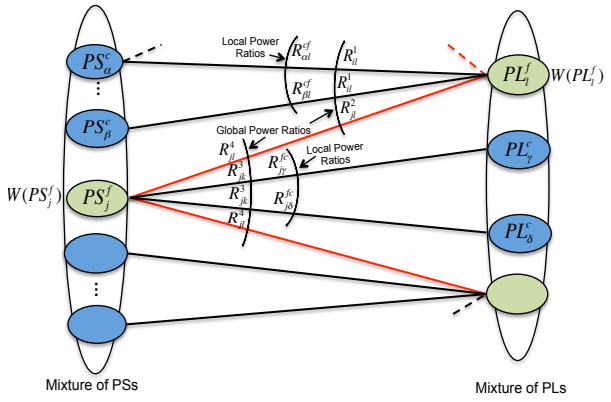

Fig. 3: PFP between fluctuating PSs and PLs.

where, P_{il}^{cf} denotes the nominal power level and R_{il}^{1} shows ratio computation of sector 2 with global aspect.

$$R_{jl}^{2} = \left[\frac{P_{jl}^{ff}}{\sum_{i=1}^{I} P_{il}^{cf} + \sum_{j=1}^{J} P_{jl}^{ff}} \right] \tag{3b}$$

where, P_{jl}^{ff}, represents the nominal power level and R_{jl}^{2} shows ratio computation of sector 4 with global aspect. Similarly, the re-computation of *GPCR* includes compilation of sector 3 and 4 and neglect the sector 2. The computation consists of two ratios; the first ratio, R_{jk}^{3}, is used for sector 3, and second ratio, R_{jl}^{4} is applied on sector 4.

$$GPCR = \begin{bmatrix} R_{jk}^{3} & R_{jl}^{4} \end{bmatrix} \tag{4}$$

$$R_{jk}^{3} = \left[\frac{P_{jk}^{fc}}{\sum_{k=1}^{K} P_{kl}^{fc} + \sum_{l=1}^{L} P_{jl}^{ff}} \right] \tag{4a}$$

where, P_{jk}^{fc} shows the nominal power level and R_{jk}^{3} is a computation of power ratio globally (with both types of PLs).

$$R_{jl}^{4} = \left[\frac{P_{jl}^{ff}}{\sum_{k=1}^{K} P_{kl}^{fc} + \sum_{l=1}^{L} P_{jl}^{ff}} \right] \tag{4b}$$

where, P_{jl}^{ff} denotes the nominal power level and R_{jl}^{4} is power ratio computation with global aspect.

After the computation of global power ratios, the resultant matrix is used for power control algorithm 5. The compiled resultant matrix is called *Power Flow Specification (PFS)*, the size of this matrix is same as the original PFP matrix with 4 sectors. The first sector of PFS matrix is same as first sector of PFP matrix while sectors 2 and 3 are re-computed with global ratios as R_{il}^{1} and R_{jk}^{3}. Sector 4 uses two power ratios for each element as, R_{jl}^{2} and R_{jl}^{4}.

The target power flow streams, power ratio computation and ratio application can be explained with the help of Fig. 3, which shows two power flow streams between fluctuating power devices. Let PS_j^f be fluctuating PS which supplies power to two fluctuating PLs. According to constraint that each fluctuating power device on both sides of the power flow must be directly attached with at least one controllable power device, the controllable power devices are attached as PS_{α}^{c}, PS_{β}^{c}, PL_{γ}^{c}, PL_{δ}^{c} and so on. The power level is assigned to each power device based on global ratio computations. As, each

Algorithm 5 For power flow between PS_j^f and PL_l^f

for $k = 1$ to K **do**
  for $j = 1$ to J such that $\exists\ l,\ P_{jl}^{ff} \neq 0$ **do**
    $W(PL_k^c) = R_{jk}^{3} \cdot W(PS_j^f) + W(PL_k^c)$
  end for
end for
for $i = 1$ to I **do**
  for $l = 1$ to L such that $\exists\ j,\ P_{jl}^{ff} \neq 0$) **do**
    $W(PS_i^c) = R_{il}^{1} \cdot W(PL_l^f) + W(PS_i^c)$
  end for
end for
for $j = 1$ to J **do**
  for $l = 1$ to L such that $P_{jl}^{ff} \neq 0$ **do**
    if $R_{jl}^{4} \cdot W(PS_j^f) \neq R_{jl}^{2} \cdot W(PL_l^f)$ **then**
      $W_{min} = Min\Big(R_{jl}^{4} \cdot W(PS_j^f), R_{jl}^{2} \cdot W(PL_l^f)\Big)$
      $W_j^{diff} = R_{jl}^{4} \cdot W(PS_j^f) - W_{min}$
      $W_l^{diff} = R_{jl}^{2} \cdot W(PL_l^f) - W_{min}$
      if $W_j^{diff} > W_l^{diff}$ **then**
        for $k = 1$ to K **do**
          $W(PL_k^c) = R_{jk}^{fc} \cdot W_j^{diff} + W(PL_k^c)$
        end for
      else
        for $i = 1$ to I **do**
          $W(PS_i^c) = R_{il}^{cf} \cdot W_l^{diff} + W(PS_i^c)$
        end for
      end if
    end if
  end for
end for

power flow between fluctuating power devices has two global power ratios (e.g., R_{jl}^{2} and R_{jl}^{4} in Fig. 3) which introduces a conflict of power levels for the given power flow. In order to solve this power levels conflict caused by two power ratio for same power flow, the difference of power supply and consumption is computed by taking minimum power level. The attached controllable power device with higher power difference compensates for power imbalance according to local power ratios (i.e., PSR/PCR calculated during compilation of sector 2 and 3). For each power flow between fluctuating devices, algorithm 5 is used to compute power levels for controllable devices when PFP and measured power levels of fluctuating devices, $W(PS_j^f)$ and $W(PL_l^f)$, are given.

In case of multiple power flow streams between fluctuating power devices, the system solves conflict one after the other. Additionally, if a fluctuating power device has multiple connections with other devices on the other side of the power flow, the assignment of power levels for fluctuating power devices is assigned first than controllable power devices. The remaining power would be assigned to controllable power devices. Note that, this is conflict resolution for static system. For practical situations, we need a dynamic system protocol which can realize this static algorithm for power flow coloring.

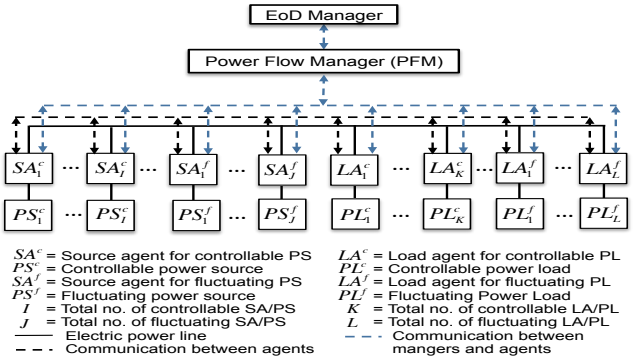

Fig. 4: System architecture.

IV. System Architecture

This section presents system architecture for implementation of the power flow coloring system over a NG (Fig. 4). The proposed system is applicable to a NG (e.g., in a house, building or local community), which consists of power managers, power agents, multiple PSs and PLs with both types i.e., controllable and fluctuating. All PSs and PLs are connected with a common electric power line. A power agent is attached to each PS/PL, which measures and controls power levels of attached power device. The power agents attached with controllable power devices (PSs/PLs) are called controllable source agent (SA^c)/load agent (LA^c). Similarly, the power agents associated with fluctuating devices (PSs/PLs) are named as fluctuating source agent (SA^f)/load agent (LA^f).

All power agents cooperate with each other for the realization of the power flow coloring system. The proposed system is a distributed system, which manages two types of communication (i) between managers and power agents, and (ii) between all power agents. To maintain, specify, and monitor the overall PFP, two types of power managers are introduced: energy on demand (EoD) manager and power flow manager (PFM). The EoD manager is responsible for maintaining power profiles of PS/PL and conducting overall power management. Each profile contains characteristics of power device i.e., minimum and maximum limitation of power levels, maximum no. of power flows that a power device can handle, and availability of a power device at particular time. The EoD manager receives *Power Demand Requests (PDRs)* from all PLs. Based on received PDRs, it mediates all power demands based on the EoD Protocol and designs a consistent PFP specifying which PS should supply how many Watts to which PL. As for the EoD protocol see [18], [19]. Then, PFP is forwarded to PFM which monitors and coordinates all power agents to maintain specified PFP. To bridge between nominal and physical power levels, PFM compiles the given PFP matrix and computes PFS matrix which then broadcast to all power agents so that the power ratios are preserved and power flow coloring system realized.

V. System Protocol

This section describes the system protocol for the implementation of the power flow coloring system in practical situations. In real world scenario, it is required to manage power fluctuations by fluctuating PSs and PLs. Here, power fluctuations include three types of fluctuations: noisy fluctuations, power variations, and power mode changes. Noisy fluctuations are physical power fluctuations due to the nature of the fluctuating PSs and PLs. The power variations occur due to the internal feedback control of the power devices and change in power levels due to low power to/from high power. The power mode changes observe due to the transient behavior of power devices (e.g., ON/OFF status change) or triggered by the EoD manager etc.

For implementation of power fluctuation management, a time-slot based feedback control (TSBFC) method is introduced. The TSBFC method preserves PFS designed by PFM. That is, TSBFC method can keep power ratios even if power fluctuations are caused by transient behaviors, nature of power devices, or mode change operations. The management of power fluctuations leads us to other problems to be solved. That is, a stability controller is required to maintain voltage stability of the NG against physical power fluctuations. For this purpose, the master and slave role assignment scheme is introduced among controllable SAs. Another expansion is required to cope with the real world scenario because electric devices operate continuously without any break. As will be described later, the TSBFC method can be designed in a way to hide communication and computation delays. Finally, the proposed system protocol can satisfy above requirements for the implementation of the power flow coloring system with fluctuating PSs and PLs in real world.

A. Stability Controller

The power fluctuations caused by PSs and PLs can make the NG unstable leading to power blackout. To maintain voltage stability of the NG against power fluctuations, one of the controllable SAs is selected as master that works as voltage and phase sources. Master SA supplies and absorbs active power (fluctuation) to keep the voltage level of the NG. The internal power control device as well as its corresponding controllable PS should be equipped with enough physical functions and power supply capacity to fulfil the role of master PS e.g., utility power line and a large storage battery. Note that, while the current implementation is designed for an AC power, it manages the active power alone and is to be revised to manage the reactive power.

All other controllable source agents operate as slaves. They work as active power sources/loads and supply/consume specified powers. How to compute and modify the power specification for each slave SA^c/LA^c based on the given PFS, which will be described later. As for the physical implementation of master and slave, refer to the section V. Note that, the master SA does not take care about specified supplying power. Additionally, when the entire power system includes multiple PSs which are capable to work as master SA, the role of master can be switched dynamically based on power system management policy, reserved for future study.

B. Time-slot Based Feedback Control (TSBFC) Method

The proposed method is developed to solve remaining problems: cope with unexpected power fluctuations of PSs and

PLs while keeping the PFS. Also, the overlay execution of time slots make the power system work continuously without being effected by communication and computation delays. Hence, TSBFC is developed to solve these problems in a systematic way. Note that, proposed TSBFC is conducted by all slave power agents and no explicit power control to comply with the PFS is conducted by the master SA.

1) Time-Slot and Protocol Description: The protocol consists of three phases; initialization phase (IP), operation phase (OP), and modification phase (MP). The EoD manager starts IP by computing PFP and send it to PFM. Then, PFM computes PFS and broadcasts it to all power agents. This message is used for the synchronization between all power agents. After that, OP starts by all power agent to implement assigned power flow specifications. The MP will start when any power agent observes an event that requires change in PFS. The event could be any change in user's behaviors , change in power consumption or supply . After observing such events, the power agent sends a CHANGE PFS message to EoD manager, which then designs a new PFP to cope with reported event and forwards it to PFM. Finally, a new OP is started by PFM. Note that, the first OP will start after IP, other OPs will execute in parallel with IP's and MP's because power devices supply/consume power continuously without any break.

At first, the time axis is divided into fixed length time-slots (TSs). In Fig. 5, OP is represented by a series of $\text{TS}_t(t = 0, 1, 2, \cdots)$. The first TS of OP is TS_0, during this TS first sector of PFS matrix is solved. That is, all power flow streams between controllable devices are fixed. In order to reduce the risks of sharp power peaks by turning ON devices, all controllable power devices start supplying or consuming power in pair one after other. In this TS, all controllable PSs and PLs reached some power level. In TS_1, all power agents with both types just measure power supply and consumption by their corresponding power devices.

During TS_2, each power agent associated with fluctuating power device sends its measured power (supply/consumption) to attached controllable power device(s). That is, all power flow streams between controllable and fluctuating power devices would be solved in this TS. In case of power flow streams between fluctuating power devices, both fluctuating power devices exchange their measured power levels with each other. This exchange of power levels is done by message transmission. The message transmission from fluctuating SA is shown by *source measured power (SMP)* while from fluctuating LA is shown as *load measured power (LMP)* in Fig. 5. Upon receiving measured information of previous TS (i.e., TS_1), each controllable agent computes power level for attached controllable power device to supply/consume in the next TS (i.e., TS_3). For power flow streams between fluctuating power devices, each fluctuating power agent saves this information to monitor behavior of other fluctuating device and also computes difference between received and its own measured power level by taking the minimum power level. Then, fluctuating power device with higher difference sends this power difference to attached controllable power agent(s). The attached controllable power agent(s) compensates for the power imbalance by computing new power level. Meanwhile,

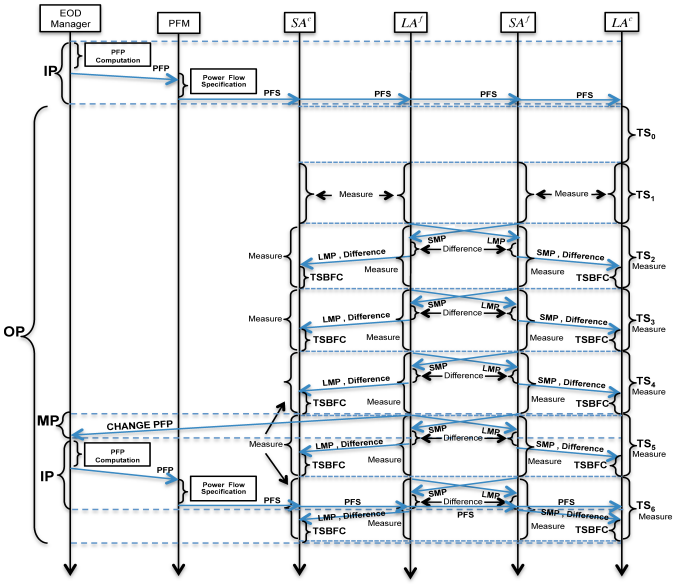

Fig. 5: System protocol.

the power measurement is continued in TS_2 in parallel with communication and computation of power levels. Note that, no power control is conducted for TS_0, TS_1, and TS_2.

In TS_t, $t \geq 3$, message exchange and computation of power levels for controllable power devices are conducted while the power measurement also continued. Note that, power control would be done in TS_3 for the measured power data of TS_1.

2) Feedback Control Method: The feedback control method is used by each slave agent to compute target power for TS_t $t \geq 3$, which implements power control to maintain specified PFS against unexpected power fluctuations of PSs and PLs. Note that, algorithm processes average power consumption and supply levels in TS_t instead of instantaneous power levels. Let $W(SA_i^c, t)$ and $W(SA_j^f, t)$ be the average measured power levels by controllable and fluctuating SAs in TS_t. Similarly, $W(LA_k^c, t)$ and $W(LA_l^f, t)$ are the average measured power levels by controllable and fluctuating LAs in TS_t.

The implementation of feedback control considers remaining sectors of PFS matrix which includes fluctuating power devices i.e., sector 2, 3 and 4. To solve sector 2 and 3, controllable power devices compute power levels by adding ratio based power of associated fluctuating power devices with algorithm 3 and 4. Here, It is assumed that there are no control errors for controllable power devices to supply or consume computed power levels accurately.

For power flow streams between fluctuating devices, there is a need to evaluate the difference between actual and measured power levels in TS_{t-2} by taking the minimum power level, $W(min, t-2)$. Both fluctuating devices compute power difference which is denoted as, $W(SA_j^{diff}, t)$ and $W(SA_l^{diff}, t)$ which shows power difference computed by jth fluctuating SA and lth fluctuating LA in TS_t. The computations are given as,

$$W(SA_j^{diff}, t) = \sum_{j=1}^{J} R_{jl}^4 \cdot W(SA_j^f, t-2) + W(SA_j^{diff}, t-2) - W(min, t-2) \quad (5)$$

$$W(LA_l^{diff},t) = \sum_{l=1}^{L} R_{jl}^2 \cdot W(LA_l^f, t-2) + W(LA_l^{diff}, t-2) - W(min, t-2) \quad (6)$$

Where, R_{jl}^4 and R_{jl}^2 are GPSR and GPCR, respectively. Based on the higher difference, attached controllable device will compensate for power imbalance, which is implemented in next TS. The calculations of power level are given as,

$$W(SA_i^c,t) = \sum_{l=1}^{L} R_{il}^{cf} \cdot W(LA_l^{diff}, t-2) + \sum_{l=1}^{L} R_{il}^{cf} \cdot W(LA_l^f, t-2) + W(SA_i^c, t-2) \quad (7)$$

$$W(LA_k^c,t) = \sum_{j=1}^{J} R_{jk}^{fc} \cdot W(SA_j^f, t-2) + \sum_{l=1}^{L} R_{jk}^{fc} \cdot W(SA_l^f, t-2) + W(LA_k^c, t-2) \quad (8)$$

Note that, computation of power levels for controllable devices is done based on local power ratio (i.e., R_{il}^{cf} and R_{jk}^{fc}). As noted before, when the PFS is modified then a new OP will start from TS_t, some inter operation phase compensation process should conducted, which is reserved for future study. When the EoD manager wants to change PFS, it has to evaluate gaps between nominal and physical power based on the previous PFS and conduct some compensation process before designing a new PFS.

VI. Experimental Results

The simulation results presented in this section verify that the proposed system works in real physical environments by (i) managing all possible power flow streams (ii) preserving local power ratios against power fluctuations, (iii) accommodating communication and computation delays, and (iv) maintaining voltage stability of the entire system. For implementation, hardware devices are developed for power sensing and control i.e., power distributer and smart tap. A power distributer consists of a microprocessor, a bidirectional AC-DC converter, and Zigbee wireless communication device. For technical details, please refer to [20]. The real-time (i.e., 16.3 msec control interval) PWM control is conducted to make it work both as voltage source (master PS) and as power source (slave PS). Smart taps are power sensors with embedded microprocessors and ZigBee wireless communication devices [10].

The detailed power fluctuations of PSs and PLs are measured by oscilloscope. All power agents associated with controllable PSs except master work as slaves. The phase and frequency control can be done both in a grid connected or a grid-off mode. Figs. 6 and 7 illustrate physical and experimental settings for grid-off mode operation of our system.

In this experiment four DC storage batteries via power distributer, a TV and a fan via smart taps are connected to a common AC 100V power line. One of the storage batteries is selected as master (i.e., PS_1^c), second emulates as a PV power source (i.e., PS_1^f) which supplies fluctuating, third is used as slave (i.e., PS_2^c), and remaining one is use as controllable PL (i.e., PL_1^c). As for the PV, storage battery is used as an emulator instead of real PV generator, which is responsible

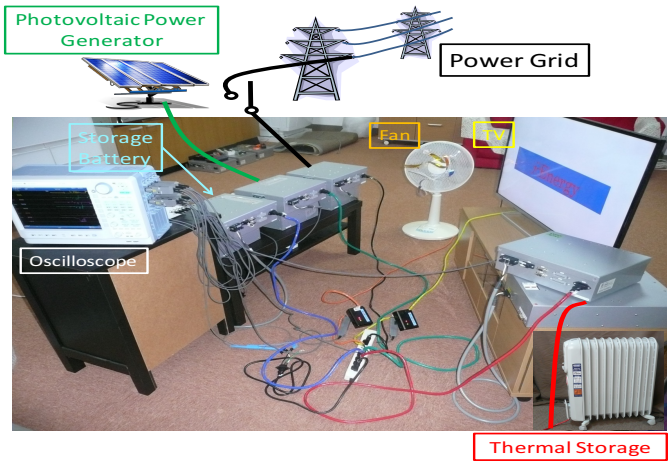

Fig. 6: Physical experiment setup.

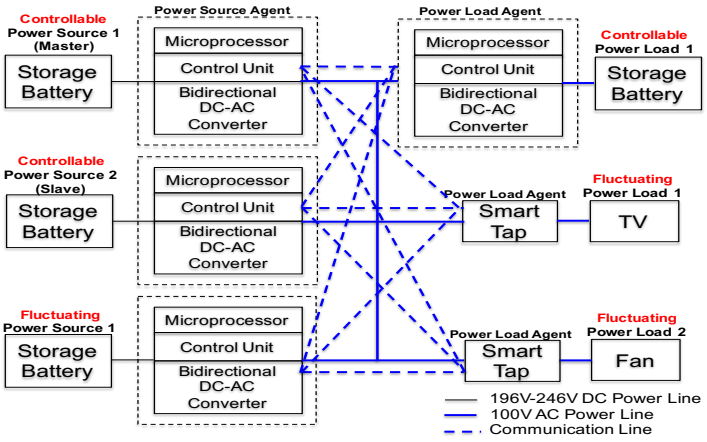

Fig. 7: Experiment setup.

for supplying power based on user-defined values for each second. These user-defined values resembles dynamics of real PV system. Additionally, we used smart TV embedded with processing unit and memory for advanced functionalities.

In this experiment, the role of master and slave to power devices, PFP, and PFS are assigned manually. That is, there are no EoD manager and PFM in this experimental setup. The PFP and power ratio computations (both global and local ratios) in PFS are given as,

$$PFP = \begin{array}{c} \\ PS_1^c \\ PS_2^c \\ PS_1^f \end{array} \begin{array}{c} \begin{array}{ccc} PL_1^c & PL_1^f & PL_2^f \end{array} \\ \begin{bmatrix} 50W & 20W & 45W \\ 50W & 15W & 45W \\ 50W & 15W & 90W \end{bmatrix} \end{array}$$

$$PFS = \begin{array}{c} \\ PS_1^c \\ PS_2^c \\ PS_1^f \\ \\ PCR \end{array} \begin{array}{c} \begin{array}{ccc} PL_1^c & PL_1^f & PL_2^f \end{array} \\ \left[\begin{array}{c|cc} 50W & 20/35 & 45/90 \\ 50W & 15/35 & 45/90 \\ \hline 50/50 & \begin{array}{c}(15/50)\\(15/155)\end{array} & \begin{array}{c}(90/180)\\(90/155)\end{array} \end{array}\right] \end{array} \begin{array}{c} \\ PSR \\ GPSR \\ GPCR \end{array}$$

Here, PL_1^f is presented as a TV, and PL_2^f is a fan. The total time

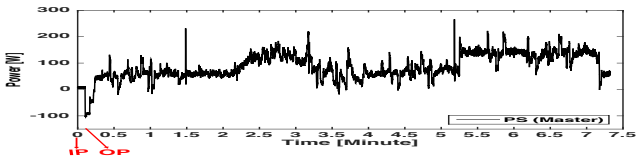

Fig. 8: Power supply of Master PS.

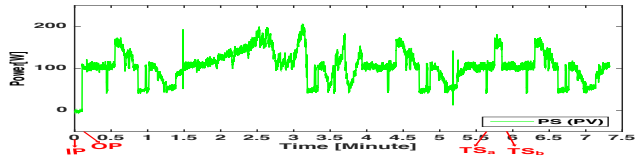

Fig. 9: Power supply of PV source.

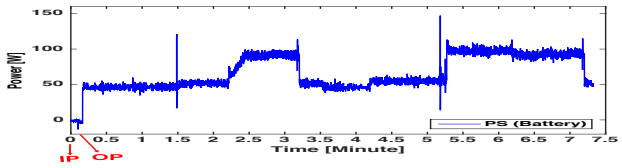

Fig. 10: Power supply of battery PS.

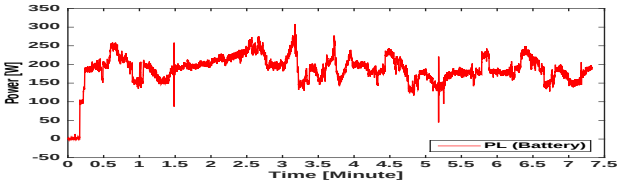

Fig. 11: Power consumption of battery PL.

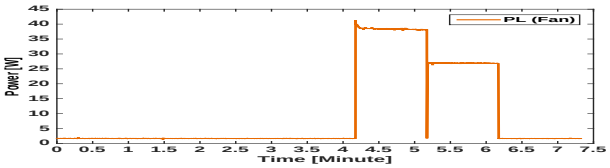

Fig. 12: Power consumption of Fan.

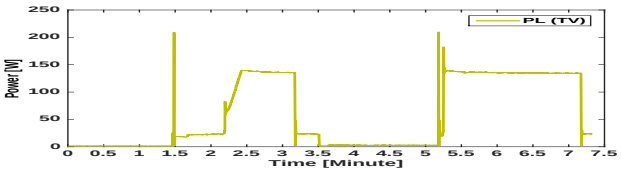

Fig. 13: Power consumption of TV.

duration of experiment is 7 minutes. The time-slot duration for feedback control is fixed to TS$= 1second$.

The starting time or IP when time,$t = 0$ (marked in graphs), all devices are switched OFF. During IP, all power agents are well synchronized based on AC cycle of 60 Hz. Then, OP started (marked in graphs) in which all PSs (Figs. 8, 9, and 10) and PLs (Figs. 11, 12, and 13) start supplying and consuming power according to PFS. Note that, fluctuating PLs i.e., TV and fan are intentionally switched OFF in the beginning of the experiment to observe the power flow streams between controllable power devices.

According to the PFS, PS_1^c and PS_2^c should supply $50W$ to PL_1^c. Fig. 10 shows that the slave PS is supplying specified power to PL_1^c where master PS supplied $50W$ to the same PL and also absorbed power fluctuations by PV. As described in previous section, power control is conducted for controllable power devices after two TSs, the power supply by PV is absorbed by master PS for the first two TSs of the OP. From TS_3, PL_1^c absorbed power supply by PV rather than master.

At time, $t = 1.5$, TV is initially connected to AC voltage (see Fig. 13). It took a brief moment for inductors and capacitors to get charged to where they react steadily with the alternating current. The power consumption of TV experienced sharp peak due to inrush current which, however rapidly died down. After this warming up period, the TV is switched ON manually for one minute. At switched OFF time power consumption of stand by mode is observed. All three PSs supplied ratio based power to TV according to PFS. Since the power consumption by TV changes largely, the power supply by PSs oscillate accordingly. Then master SA_1^c automatically stabilizes (absorbs) the oscillation by maintaining the voltage level of the NG. Hence, no oscillation is observed in the power consumption TV as shown in Fig. 13. After that fan is switched ON manually and remained ON for one minute with strong operating mode (see Fig. 12). The operating mode of fan is shifted to weak mode for one more minute and TV is switched ON at the same time (see Fig. 13). The TV remained switched ON for two minutes. This shows all power devices are operating, which shows power flow streams.

In order to show the correctness of our proposed algorithm in managing power flow streams between fluctuating power devices, two quantitative analysis are presented in Figs. 14 and 15. We choose two extreme points (marked as TS_a and TS_b in Fig. 9) which show high and low PV generation. In Fig. 14 (high PV generation is discussed), power levels are assigned to fluctuating power devices according to GPSR and GPCR (calculate in black in Fig. 14). Note that, the measured power levels for fluctuating devices are taken two TSs before from the recorded data of the experiment i.e., MP_{a-2}. We got these power levels from log file created during experiment. At first, the power flow stream between PS_1^f and PL_1^f would be solved. The conflict of assigned power levels for this particular power flow is solved by taking the difference (calculated in red). The difference of power levels is higher at PL_1^f side. So, this difference is distributed among attached controllable power devices i.e., PS_1^c and PS_2^c based on local power ratios (computed in blue) in Fig. 14. Also, the difference of power levels for power flow between PS_1^f and PL_2^f is compensated by PL_1^c as this is only attached controllable device. The compensation is added to the new target power level for controllable power devices as TP_a (computed for all controllable devices in Fig. 14). This computation show that the target power in current TS based on measured data of two TSs before is nearly same. This analysis also proves that the power supply to a specific load from multiple sources can be realized stably, i.e., no power oscillations are observed in

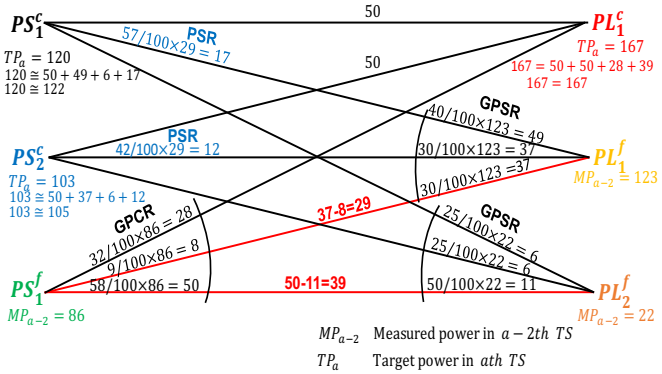

Fig. 14: Power fluctuation management with low PV power.

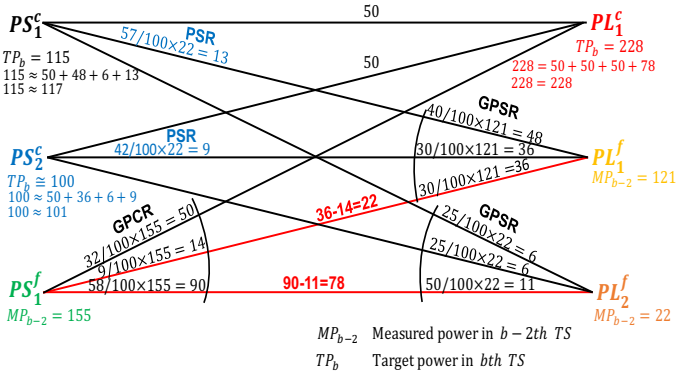

Fig. 15: Power fluctuation management with high PV power.

power consumption of TV and fan (Fig. 12 and Fig. 13) and local power ratios are preserved as shown in calculations for controllable power devices. From these calculations, we can see that the specified PSR and PCR are maintained accurately against large power variations of fluctuating power source.

Finally, we measured fluctuations of effective voltage at shared power bus to show the effectiveness of voltage stability control by master SA working as voltage source (see Fig. 16). We obtained the following statistical measures: number of measured samples: 43,95,582, average: 99.974V, min: 97.412V, max: 101.1000V, and standard deviation: 0.1313V. These measures verified that the voltage of power bus line is maintained stably.

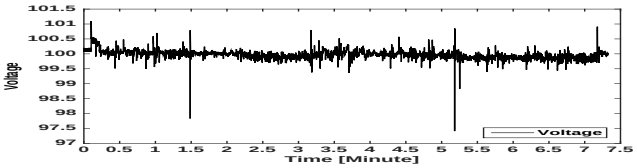

Fig. 16: Voltage stability.

VII. Concluding Remarks

In this paper, a cooperative distributed control method is proposed to implement the power flow coloring system over a NG with fluctuating power sources and loads while keeping the voltage stability of the NG. The experimental results demonstrated that the proposed method can (i) maintain voltage stability (ii) keep the specified power ratios against power fluctuations (iii) accommodate communication and computation delays. For the implementation in real environment, the proposed system should be modified in following ways: (1) an inter operation phase for power compensation is required for long run operation including change in PFP, (2) how to change the role of master and slave during system operation, (3) how to manage reactive power, (4) how to handle noise and ambiguous data, and finally (5) system ability to handle fail-safe problems.

Acknowledgment

This work was supported by JSPS Grants-in-Aid (KAKENHI) Grant Number JP16K12394 and i-Energy Joint Research Chair in Kyoto University.

References

[1] E. Harrison, D. Saad, and K. Y. M. Wong, "Message passing for distributed optimisation of power allocation with renewable resources," *2nd Int. Conf. on Intelligent Green Building and Smart Grid (IGBSG)*, pp. 1-6, 2016.

[2] D. Brown, and C. Koravos (2014), *Japan's FIT: Flying too close to the sun?*, [Online]. Available: https://www.dlapiper.com/media/Files/Insights/Publications/2014/10/Japans-fit.

[3] N. Y. Dahlan, M. A. Jusoh, and W. N. A. W. Abdullah, "Solar grid parity for Malaysia: analysis using experience curves," *IEEE 8th Power Eng. and Optimization Conf. (PEOCO)*, pp. 641-466, 2014.

[4] E. Eusebio, and C. Camus, "Residential PV systems with battery backup power attained already grid parity?," *13th Int. Conf. on the European Energy Market (EEM)*, pp. 1-5, 2016.

[5] M. H. Shwehdi, and S. R. Muhammad, "Proposed smart DC Nano-Grid for green buildings a reflective view," *Int. Conf. on Renewable Energy Research and Applicat. (ICRERA)*, pp. 765-769, 2014.

[6] M. C. Kinn, "Proposed components for the design of a smart Nano-Grid for a domestic electrical system that operates at below 50V DC," *IEEE PES Int. Conf. and Exhibition on Innovative Smart Grid Tech. (ISGT Europe)*, pp. 1-7, 2011.

[7] W. Zhang, F. C. Lee, and P. Y. Huang, "Energy management system control and experiment for future home," *IEEE Energy Conversion Congr. and Exposition (ECCE)*, pp. 3317-3324, 2014.

[8] N. Hatziargyriou, H. Asano, R. Iravani, and C. Marnay, "Microgrids," *IEEE Power and Energy Mag.*, vol. 5, no. 4, pp. 78-94, 2007.

[9] T. Matsuyama: "Creating safe, secure, and environment-friendly lifestyles through i-Energy," *New Breeze*, vol. 21, no. 2, pp.1-8, 2009.

[10] T. Matsuyama: "i-Energy: Smart demand-side energy management," Chapter 8, *Smart Grid Applicat. and Develop.*, Springer, 2014.

[11] S. Javaid, Y. Kurose, T. Kato, and T. Matsuyama, "Cooperative distributed control implementation of the power flow coloring over a nano-grid with fluctuating power loads," *IEEE Trans. on Smart Grid*, pp. 1-11, 2016.

[12] D. Forfia, M. Knight, and R. Melton, "The view from the top of the mountain: Building a community of practice with the gridwise trasactive energy framework," *IEEE Power and Energy Magazine*, vol. 14, no. 3, pp. 25-33, 2016.

[13] K. Kok, and S. Widergren, "A society of devices: Integrating intelligent distributed resources with transactive energy," *IEEE Power and Energy Magazine*, vol. 14, no. 3, pp. 34-45, 2016.

[14] Y. Okabe and K. Sakai, "QoEn (quality of energy) routing toward energy on demand service in the future internet," *The Inst. of Electr., Inform. and Comm. Eng.* Tech. Report no. IA2009-47(2009-10), 2009.

[15] T. Takuno, Y. Kitamori, R. Takahashi, and T. Hikihara, "AC power routing system in home based on demand and supply utilising distributed power sources," *Energies*, pp. 717-726, 2011.

[16] R. Abe, H. Taoka and D. McQuilkin, "Digital Grid: communicative

electrical grids of the future," *IEEE Trans. on Smart Grid*, vol. 2, no.2, June 2011.
[17] R. Takahashi, K. Tashiro, and T. Hikihara, "Router for power packet distribution network: Design and experimental verification," *IEEE Trans. on Smart Grid*, vol. 6, no. 2, pp. 618-626, 2015.
[18] T. Kato, K. Yuasa, and T. Matsuyama, "Energy on demand: efficient and versatile energy control system for home energy management," *Proc. SmartGridComm2011*, pp. 410-415, 2011.
[19] T. Kato, K. Tamura, and T. Matsuyama, "Adaptive storage battery management based on the energy on demand protocol," *Proc. SmartGridComm2012*, pp. 43-48, 2012.
[20] T. Edagawa, K. Fukae, and T. Hisakado, "Peer-to peer energy transmission system by bidirectional AC-DC converter module," *Inst. of Elect. Eng. of Japan*, Tech. Rep. PE-14-191, PSE-14-191, 2014 (In Japanese).

Saher Javaid Saher Javaid received Bachelor's degree in Computer Science and Master's degree in Information Technology from Allama Iqbal Open University, Islamabad in 2004 and University of the Punjab, Lahore, Pakistan in 2007, respectively. She received Ph.D. degree in Information Science from Japan Advanced Institute of Science and Technology in 2014. Since 2014, she has been working as assistant professor in Kyoto University. Her research interests include distributed sensing and control and smart energy management systems.

Takekazu Kato Takekazu Kato received his BS, and DS degree in Okayama University, Japan, in 1997, and 2001, respectively. He is currently a associate professor in the Graduate School of Informatics, Kyoto University. His research interests include pattern recognition, computer vision, and energy management. He is a member of IEEE, IEEE Communications Society, IPSJ, and IEICE.

Takashi Matsuyama Professor Takashi Matsuyama received B. Eng., M. Eng., and D. Eng. degrees in electrical engineering from Kyoto University, Japan, in 1974, 1976, and 1980, respectively. He is currently a professor in the Department of Intelligence Science and Technology, Graduate School of Informatics, Kyoto University.

He studyied cooperative distribute sensing-control-reasoning systems over 30 years. Their application fields include knowledge-based image understanding, visual surveillance, 3D video, human-computer interaction, and smart energy management. He wrote more than 100 journal papers and more than 20 books including three research monographs.